Chemical Engineering Journal 156 (2010) 298–304

Contents lists available at ScienceDirect

Chemical Engineering Journal

journal homepage: www.elsevier.com/locate/cej

# Application of two sites non-equilibrium sorption model for the removal of Cu(II) onto grape stalk wastes in a fixed-bed column

Antonio Florido, César Valderrama*, Jaime A. Arévalo, Ignasi Casas, María Martínez, Nuria Miralles

*Departament d'Enginyeria Química, ETSEIB, Universitat Politècnica de Catalunya, 08028 Barcelona, Spain*

ARTICLE INFO

*Article history:*
Received 5 June 2009
Received in revised form 5 October 2009
Accepted 6 October 2009

*Keywords:*
Grape stalk wastes
Cu
Sorption
Breakthrough curve
Two-site non-equilibrium sorption model

ABSTRACT

Grape stalk wastes generated in the wine production process were used for the removal of Cu(II) from aqueous solutions. Column experiments were performed and the code CTXFIT (two-site non-equilibrium sorption model) was used in order to fit the experimental data and to determine the sorption and transport parameters. The effects of both inlet metal concentration and the particle size were evaluated. The retention capacity of the compacted bed was affected by the initial metal concentration as well as the transport and sorption parameters. Columns with higher inlet concentration were fast saturated leading to shorter breakthrough and exhaustion times. The maximum retardation factor ($R$) was observed for the particle size of 0.35–0.5 mm. A clear decrease in that parameter was observed for larger particle size, and for the small particle sizes high flow resistance was observed and lower values of $R$ were reported. The recovery of the metal in desorption experiments was close to 85%.



## 1. Introduction

Contamination by hazardous heavy metals like copper has become a serious environmental problem of worldwide concern [1]. Several industries, for example, dyeing, paper, petroleum, copper/brass plating and copper–ammonium rayon, release undesired amounts of Cu(II) ions. In the copper-cleaning, plating and metal-processing industries, Cu(II) concentrations approach 100–120 mg $L^{-1}$, respectively [2]. Aside from the environmental damage, human health is likely to be affected as the presence of heavy metals beyond a certain limit brings serious hazards to living organisms, for instance Cu(II) has been proved to cause liver damage or Wilson disease [3]. It is also toxic to fish life even when its content is in low amounts in natural waters [4]. Considering the harmful effects of heavy metals, it is necessary to remove them from liquid wastes at least to the limit accepted by the regulations. World Health Organization (WHO) recommended a maximum acceptable concentration of Cu(II) in drinking water of 1.5 mg $L^{-1}$ [5]. Many technologies have been employed to remove heavy metal ions from wastewater, including precipitation, flotation, ion exchange, membrane-related process, electrochemical technique and biological process [3,6]. These conventional techniques can reduce metal ions, but they do not appear to be highly effective due to the limitations in the pH range as well as the high material and operational costs [5]. The sorption process is one of the few alternatives available for the removal of heavy metals at low concentrations from industrial effluents, regarding its simplicity and high-efficiency characteristics [7]. One of the bigger disadvantages of the sorption processes is the need of dispose or regeneration of the sorbent material. Activated carbon, activated alumina or polymer resins which are non-regenerable and expensive materials, are the sorbents usually used for this purpose [6,8,9]. The ability of biological materials to sorb metal ions has received considerable attention for the development of an efficient, clean and cheap technology for wastewater treatment at metal concentrations [10]. One of these sorbents is grape stalk wastes generated in the wine production process, which has been satisfactorily applied in copper and nickel [11,12]; lead and cadmium [13] and chromium removal [14]. In these works, sorption of Cu(II) on grape stalks released an equivalent amount of alkaline and alkaline earth metals ($K^+$, $Mg^{2+}$, $Ca^{2+}$) as well as protons, indicating that ionic exchange is predominantly responsible for metal ion uptake. Both batch and kinetic experiments showed sorption uptake to have a pH-dependent profile, with a Cu(II) maximum sorption recovery at around pH 5.5–6.0 [11].

Batch experiments are used to obtain equilibrium sorption isotherms and to evaluate the sorption capacity of sorbents for given metals present in fluid phases [15]. However, in the practical operation of full-scale biosorption processes, continuous-flow fixed-bed columns are often preferred. In such systems, the concentration profiles in the liquid and sorbent phases vary in both space and time [10,16]. As a result, it is difficult to carry out a priori design and optimization of fixed-bed columns without a quantitative approach. From the perspective of process modelling, the

* Corresponding author at: Departament d'Enginyeria Química, Universitat Politècnica de Catalunya, Av. Diagonal 647, Edifici H Planta 4ª, 08028 Barcelona, Spain. Tel.: +34 93 401 18 18; fax: +34 93 401 58 14.
*E-mail address:* cesar.alberto.valderrama@upc.edu (C. Valderrama).

1385-8947/$ – see front matter © 2009 Elsevier B.V. All rights reserved.
doi:10.1016/j.cej.2009.10.020

dynamic behaviour of a fixed-bed column is described in terms of breakthrough curve [17].

The objective of the present study is the recovery of Cu(II) from aqueous solutions by using grape stalk wastes in a fixed-bed column. The sorption capacities, the effect of the initial metal concentration, the particle size sorbent and regeneration process have been evaluated. The CXTFIT code [18] has been used to estimate the parameters of the two-site non-equilibrium convection–dispersion equation (TSM/CDE) by adjusting the model to the experimental breakthrough curves (BTC).

### 1.1. Two-site non-equilibrium sorption model

The conceptual model of chemical (two-site) non-equilibrium transport [19] regards the sorption mechanism in two steps, occurring either in series or in parallel. One is instantaneous and at equilibrium; the other is rate-limited and described by first-order kinetics. A model incorporating more than two types of sorption would be more realistic, but difficult to use in the sense of practical application. Thus, the two-site model appears to be a good balance between the degree of accuracy and field applicability. For non-linear sorption, which is assumed for both sorption domains, the non-equilibrium transport equation is expressed as [20]

$$\frac{\partial C}{\partial t} + \left(\frac{\rho}{\theta}\right)\left(\frac{\partial S_1}{\partial t} + \frac{\partial S_2}{\partial t}\right) = D\frac{\partial^2 C}{\partial x^2} - \nu\frac{\partial C}{\partial x} \quad (1)$$

where $C$ is the flux average or resident concentration (mg L$^{-1}$), $\rho$ is the sorbent bulk density (kg m$^{-3}$), $\theta$ is the volumetric water content (m$^3$ m$^{-3}$), $t$ is time ($h$), $S_1$ is the solid phase concentration on equilibrium sites (mg kg$^{-1}$), $S_2$ is the solid phase concentration on kinetic non-equilibrium sites (mg kg$^{-1}$), $D$ is the dispersion coefficient (cm$^2$ h$^{-1}$), $x$ is distance (cm) and $\nu$ is the average pore water velocity (cm h$^{-1}$).

The non-equilibrium sorption process is defined by

$$\frac{\partial S_2}{\partial t} = \alpha[(1-F)f(C) - S_2] \quad (2)$$

where $F$ represents the fraction of the sites available for instantaneous sorption and $\alpha$ is a first-order rate coefficient (h$^{-1}$). At equilibrium, sorption on both sites is described by the following non-linear isotherms [15,21,22]:

$$S_1 = Ff(C) \quad (3)$$

and

$$S_2 = (1-F)f(C) \quad (4)$$

Both transport and sorption parameters were estimated by using the CTXFIT code under flux-type boundary conditions [15,18] to fit the experimental breakthrough data. The following dimensionless form of the two-site non-equilibrium model was adjusted to the breakthrough curves:

$$\beta R\frac{\partial C_1}{\partial T} = \left(\frac{1}{P}\right)\left(\frac{\partial^2 C_1}{\partial X^2}\right) - \frac{\partial C_1}{\partial X} - \omega(C_1 - C_2) \quad (5)$$

$$(1-\beta)R\frac{\partial^2 C_2}{\partial T} = \omega(C_1 - C_2) \quad (6)$$

where the dimensionless parameters are defined as follows:

$$C_1 = \frac{C}{C_0} \quad (7)$$

$$C_2 = \frac{S_2}{[(1-F)k_L C_0]} \quad (8)$$

$$T = \frac{\nu t}{L} \quad (9)$$

**Table 1**
Physical and chemical properties of grape stalk wastes.

| Property | Grape stalks |
|---|---|
| Elemental analysis[a] (wt.%) | |
| C | 42.4 |
| H | 5.8 |
| N | 0.8 |
| S | n.d. |
| BET[b] Surface area (m$^2$ g$^{-1}$) | 0.42 |
| Total porosity (%) | 72.3 |
| Bulk density (g dm$^{-3}$) | 304 |
| Apparent density (g dm$^{-3}$) | 1101 |
| Net amount of cation released (mequiv. g$^{-1}$) due to proton uptake | |
| $Ca^{2+}$ | 0.382 |
| $Mg^{2+}$ | 0.126 |
| $K^+$ | 0.107 |
| $Na^+$ | 0.001 |
| CEC[c] (mmol g$^{-1}$) | 0.36 |

[a] Elemental Analyzer EA 1110 CE Instruments (Italy) [12].
[b] BET (Brunauer, Emmet, Teller) method.
[c] Cation exchange capacity (CEC) [11].

$$X = \frac{x}{L} \quad (10)$$

$$R = 1 + \frac{\rho k_L}{\theta} \quad (11)$$

$$P = \frac{\nu L}{D} \quad (12)$$

$$\beta = \frac{(\theta + F\rho k_L)}{(\theta + \rho k_L)} \quad (13)$$

$$\omega = \frac{\alpha(1-\beta)RL}{\nu} \quad (14)$$

In the above Eqs. (7) and (8) $C_1$ and $C_2$ (mg L$^{-1}$) are the relative concentration of metal in equilibrium and kinetic sites, respectively, scales to $C_0$ (mg L$^{-1}$); Eq. (9) $T$ is the dimensionless time and $L$ is the column length; Eq. (10) $X$ is the dimensionless distance; Eq. (11) $R$ is the retardation factor; Eq. (12) $P$ is the Peclet number; Eq. (13) $\beta$ is the fraction of instantaneous retardation and $k_L$ (m$^3$ kg$^{-1}$) is the linear isotherm sorption coefficient; and Eq. (14) $\omega$ is a dimensionless mass transfer coefficient [15,18].

## 2. Materials and methods

### 2.1. Materials

Grape stalk wastes generated in the wine production process (supplied by a wine manufacturer of the Empordà-Costa Brava region, Girona, Spain), were rinsed three times with deionised water, dried in an oven at 110 °C until constant weight, and finally cut and sieved for five particle size ranged from 0.1 to 1.0 mm. The properties of the sorbents are listed in Table 1. Metal solutions were prepared by dissolving appropriate amounts of $CuCl_2{\cdot}2H_2O$(s) in deionised water. All reagents were analytical grade and were purchased from Panreac (Barcelona, Spain). Metal standard solutions of 1000 mg L$^{-1}$ purchased from Carlo Erba (Milano, Italy) were used for Flame Atomic Absorption Spectroscopy (FAAS).

### 2.2. Characterization of the sorbent

Fourier Transform Infrared (FTIR) Analysis was performed in order to give a qualitative and preliminary analysis of the main functional groups that might be involved in metal uptake. The FTIR analysis in solid phase was performed using a Fourier Transform Infrared Spectrometer (Galaxy Series FTIR 5000, Mattson). Spectra of the sorbent before and after Cu(II) sorption process were carried out. For FTIR analysis, 300 mg KBr disks containing 3 mg of

finely grounded grape stalks were prepared. The surface structure of the grape stalks before and after Cu(II) sorption process was also analysed by scanning electronic microscopy (SEM, Jeol JSM-6400) coupled with energy dispersive X-ray analysis (EDX).

### 2.3. Sorption column experiments

For non-reactive tracers, like the $NO_3^-$ used to characterize the hydraulic conditions in this study, the CDE can be reduced to [15,23]:

$$\frac{\partial C}{\partial t} = D\frac{\partial^2 C}{\partial x^2} - v\frac{\partial C}{\partial x} \quad (15)$$

The flow regime can then be characterized by applying the tracer at the same flow rate as the solute influent. Nitrate tracer solutions were prepared by dissolving appropriate amounts of $NaNO_3$(s). Nitrate anion (100 mg $L^{-1}$) was used as a tracer previously to each column experiment in order to determine the transport parameters of the column. The tracer was pumped trough the column at the same flow rate to be used in the successive metal uptake determinations and was quantified by high performance liquid chromatography coupled with UV-diode array detector (Waters 2695).

All column experiments were conducted in duplicate in glass columns of 72 mm length and 10 mm internal diameter (Omnifit) and uniformly packed with 1.7–1.8 g of grape stalks treated as explained above. During the column sorption operation at different initial concentrations, the aqueous metal solution containing either 20 or 70 mg $L^{-1}$ of Cu(II) was pumped upwards through the column at a constant flow rate (11 mL $h^{-1}$) and grape stalks particle size of 0.8–1.0 mm, while the effect of grape stalks particle size on the fixed-bed sorption was performed at inlet Cu(II) concentration of 70 mg $L^{-1}$. Samples were collected from the outlet of the column by a fraction collector (Gilson FC204) at pre-set time intervals. The pH of the solution was monitored by using a glass electrode and the metal concentration in solution was determined by Flame Atomic Absorption Spectrometry using a Varian Absorption Spectrometer (Model 1275). The Cu(II) metal determination was performed at a wavelength of 324.8 nm

### 2.4. Desorption experiments

For any sorption process, one of the most important factors is the recovery of the sorbate material and regeneration capacity of the sorbent. Although, in the present work the recovery of the sorbate is clearly not an issue because of its nature, the knowledge of this process can give an important insight on the understanding of the overall mechanism of sorption. Consequently, experiments were carried out in which a grape stalk samples was loaded with sorbate and subjected to elution of metal ion with 0.1 M $HClO_4$ at a flow rate of 11 mL $h^{-1}$, as in the previous experiments. Samples were collected as described above, and metal concentration was determined by FAAS.

### 2.5. Breakthrough sorption capacity

The breakthrough point is chosen arbitrarily at some low value, $C_b$ (mg $L^{-1}$); and the sorbent is considered to be essentially exhausted when the effluent concentration, $C_x$ (mg $L^{-1}$), reaches the 90% of $C_0$ (initial concentration of sorbate, mg $L^{-1}$) [24–26].

The sorption zone computations are defined by the time of exhaustion $t_x$ (h) and the time of passage through the sorption zone $t_\delta$ (h).

$$t_x = \frac{V_x}{Q} \quad (16)$$

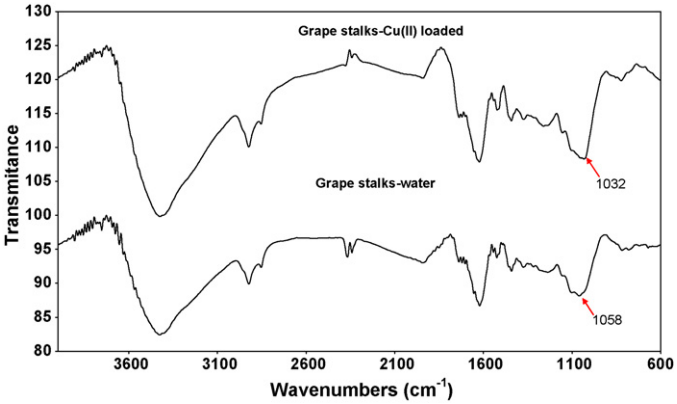


**Fig. 1.** FTIR spectra in solid phase of grape stalk wastes in KBr disk before and after the Cu(II) sorption.

$$t_\sigma = \frac{(V_x - V_b)}{Q} \quad (17)$$

where $V_x$ and $V_b$ (L) are the volumes of liquid passed through column at exhaustion and breakthrough (90% and 2% of $C_0$) respectively and $Q$ (L $h^{-1}$) is the flow rate. The velocity at which the sorption zone moves through the column is constant except during its formation. This velocity defines the sorption zone height $\delta$ (cm).

$$\sigma = \frac{L}{(t_x - t_f)}t_\sigma \quad (18)$$

where $L$ is the column height (cm) and $t_f$ (h) the zone formation time.

The capacity at exhaustion $q_{column}$ (g $kg^{-1}$) is determined by calculating the total area below the breakthrough curve. This area represents the amounts of solute sorbed by mass of solid in the sorption zone from the breakpoint to exhaustion [25–27].

$$q_{column} = \frac{\int_{V_b}^{V_x}(C_0 - C)dV}{m_s} \quad (19)$$

where $C$ is the outlet metal concentration (mg $L^{-1}$) and $m_s$ is the mass of the sorbent (g).

## 3. Results and discussion

### 3.1. Fourier Transform Infrared (FTIR) Spectroscopy

The FTIR spectra of grape stalks and grape stalks loaded with Cu(II) are presented in Fig. 1. As shown in the figure, the spectra display a number of absorption peaks, indicating the complex nature of the material examined. The broad absorption peaks around 3424 $cm^{-1}$ are indicative of the existence of hydroxyl groups of alcohols, phenol and carboxylic acids. The peaks observed at 2925 $cm^{-1}$ and 2860 $cm^{-1}$ can be assigned to the C–H groups of aliphatic acids. The peaks around 1623 $cm^{-1}$ correspond to the C=C stretching that may be attributed to the lignin aromatic C–C bond. The lignin structure can also be confirmed by the strong C–O band at 1058 $cm^{-1}$. Similar results were presented by Farinella et al. [28] with grape bagasse generated in the wine production process. This C–O band absorption peak is observed to shift to 1032 $cm^{-1}$ when grape stalks are loaded with copper. Thus, it seems that this type of functional group is likely to participate in metal binding.

### 3.2. Analysis of grape stalks by SEM-EDX

Scanning electron micrographs and spectra of grape stalks before and after sorption are shown in Fig. 2. A comparison of the

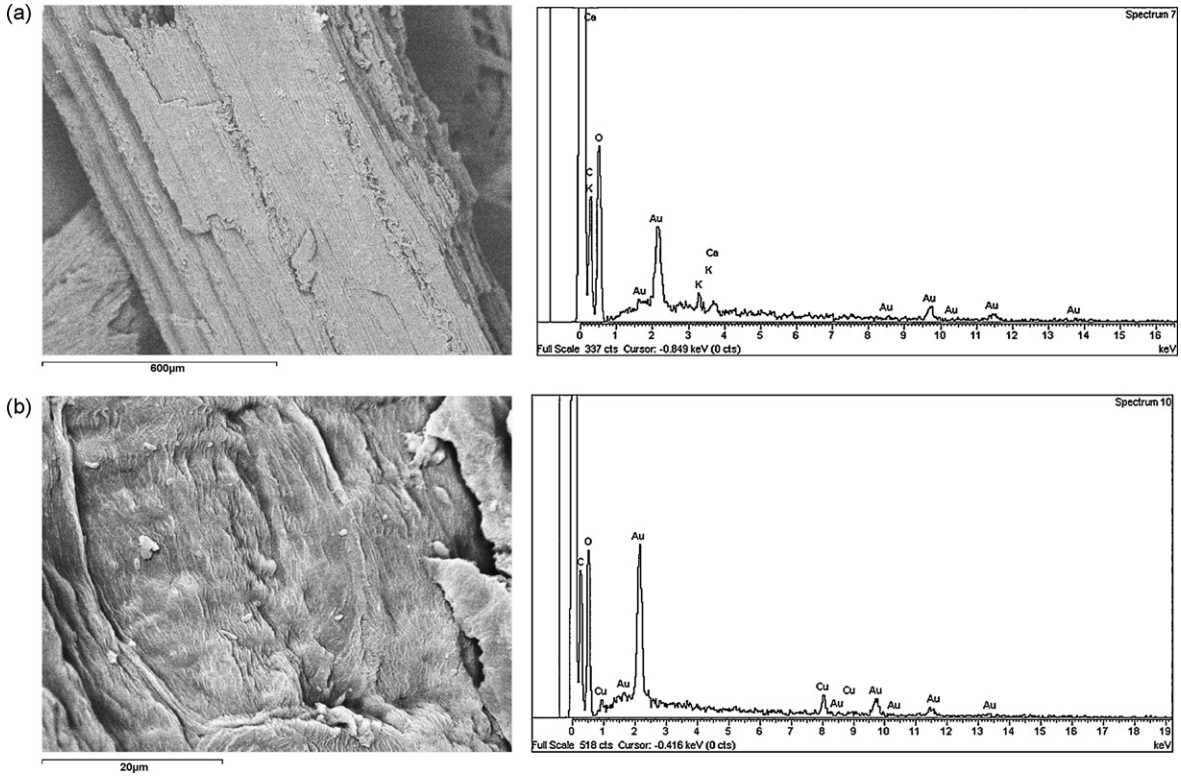


**Fig. 2.** (a) (Bar 20 μm) SEM micrograph and EDX spectra of grape stalks before loading. (b) (Bar 20 μm) SEM micrograph and EDX spectra of grape stalks after loading with cooper chloride solution (1000 mg $L^{-1}$).

grape stalks SEM images before and after the Cu(II) sorption indicates that some modifications on the grape stalks particles can be observed, thus, a strong density of pellets on grape stalks after Cu(II) loading can be observed in Fig. 2b. The pellets observed in SEM were also characterized by energy dispersive X-ray spectrometry (EDX). The EDX analysis shown in Fig. 2b reveal Cu(II) signals, on the surface of the grape stalks after metal sorption. The presence of gold peaks in all spectra is due to the gold purposely settled to make the samples conductive.

### 3.3. Effect of initial Cu(II) concentration

An increase of the initial Cu(II) concentration when other experimental conditions are kept constant, significantly affected the breakthrough curve as illustrated in Fig. 3 and parameters calculated in Table 2.

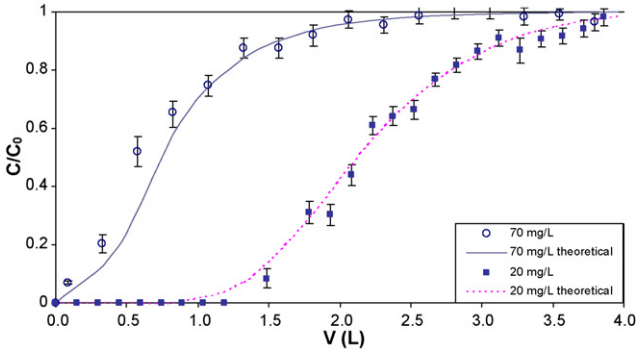


**Fig. 3.** The measured and modelled breakthrough curves for sorption of Cu(II) onto grape stalks (0.8–1.0 mm particle size) at different initial concentration (20 and 70 mg $L^{-1}$). Error bars represent one standard deviation.

When the initial Cu(II) concentration is increased from 20 to 70 mg $L^{-1}$, the corresponding sorption bed capacity appears to increase from 17 to 35 mg $g^{-1}$. A decrease in the inlet Cu(II) concentrations resulted in delayed breakthrough curves and the treated volume was also higher, since the lower concentration gradient caused slower transport due to decreased diffusion coefficient [10,29]. At the highest Cu(II) concentration (70 mg $L^{-1}$) the grape stalks column saturated faster leading to earlier breakthrough and exhaustion times.

The simulation of the breakthrough curves at different initial concentration was performed by the CTXFIT code as it has been mentioned in Section 2.3. The transport and sorption parameters are reported in Table 3. Fig. 3 shows the experimental breakthrough and the calculated values obtained by the two sites non-equilibrium sorption model. A good fit was obtained for both initial concentrations, denoting that this model describes properly the transport and sorption processes. As was expected from the breakthrough calculations the Cu(II) transport was more retarded (large $R$ values) at lower inlet concentration [20]. This behaviour was also observed (Table 3) for the parameter $\beta$, a partition coefficient which indirectly represents the fraction of the sites available for instantaneous sorption. The linear isotherm sorption coefficients as well as the first-order rate coefficient $\alpha$ were in the same order of magnitude for both inlet Cu(II) concentrations.

The pH was monitored as a function of time. The values of pH measured ranged between 6 at starting point of the experiment

**Table 2**
Fixed-bed calculations and breakthrough capacity for Cu(II) sorption onto grape stalks.

| $C_0$ | $C_x$ | $C_b$ | $V_x$ | $V_b$ | $t_x$ | $t_f$ | $q_{column}$ | $\delta$ |
|---|---|---|---|---|---|---|---|---|
| 70 | 63 | 14 | 1.60 | 0.33 | 145 | 2 | 35.07 | 4.98 |
| 20 | 18 | 0.4 | 3.10 | 1.70 | 282 | 80 | 17.04 | 3.78 |

**Table 3**
Physical parameters obtained by fitting the equilibrium CDE to the breakthrough of $NO_3^-$ tracer ($R = 1$), and model parameters obtained by fitting Cu(II) experimental breakthrough data to the non-equilibrium sorption model.

| $C_0$ | Physical parameters ($R = 1$) | | | Two-site sorption model parameters | | | | | |
|---|---|---|---|---|---|---|---|---|---|
| | $D$ | $v$ | $r^2$ | $R$ | $\beta$ | $\omega$ | $r^2$ | $k_L$ | $\alpha$ |
| 70 | 3.0 | 2.2 | 0.950 | 42.0 | 0.51 | 0.06 | 0.960 | 0.03 | 0.001 |
| 20 | 0.8 | 2.4 | 0.992 | 79.9 | 0.90 | 0.01 | 0.994 | 0.06 | 0.0005 |

until 4 when the column was exhausted. The column experiments were performed under the best pH conditions that were observed at the previous batch experiments, which reported maximum metal removal at pH 6 [11].

### 3.4. Effect of the particle size in Cu(II) sorption

The experiments were carried out for five different particle (grape stalk) sizes: 0.1–0.2, 0.2–0.35, 0.35–0.5, 0.5–0.8 and 0.8–1.0 mm, under constant flow rates (11 mL $h^{-1}$) and inlet Cu(II) concentrations (70 mg $L^{-1}$). The amount of grape stalk sorbent was kept constant (1.7–1.8 g).

It is well known that by decreasing the particle size, the performance of sorption is improved; however, small particle sizes can result in high flow resistance of the column and should be avoided [10]. Fig. 4 shows the influence of particle sizes on metal sorption. It can be seen the behaviour observed for the particle sizes larger than 0.35 mm was as expected, however for values less than 0.35, the maximum bed capacities and breakthrough time are reduced. This can be explained because the voidages of the sorption beds are reduced for the small particle size ranges [30]. A larger particle may give high interparticle voidage. Hence, for the same mass of sorbent, the column packed with the larger sorbent particle size range gives a longer column than that packed with smaller diameter sorbent particles.

In the particle size range of 0.35–0.5 mm, sorption breakthrough curves followed a much more efficient profile than for larger particle size ranges, in that the breakthrough time increased and the curves tended towards the classic "S" shape profile [31].

Tables 4 and 5 collect the breakthrough capacity and the transport and sorption parameters obtained by the non-equilibrium sorption model. As was expected the maximum bed capacity was reported for 0.35–0.5 mm particle size. For larger particle size the trend was that bed capacities, transport and sorption parameters decreased significantly with increasing particle size. This behaviour is due to the reduction of the equilibrium sorption sites available in the larger particle sizes. For the small particle sizes, a high flow resistance of the column resulted in poor sorption capacity and the parameters obtained for the non-equilibrium model were the lowest.

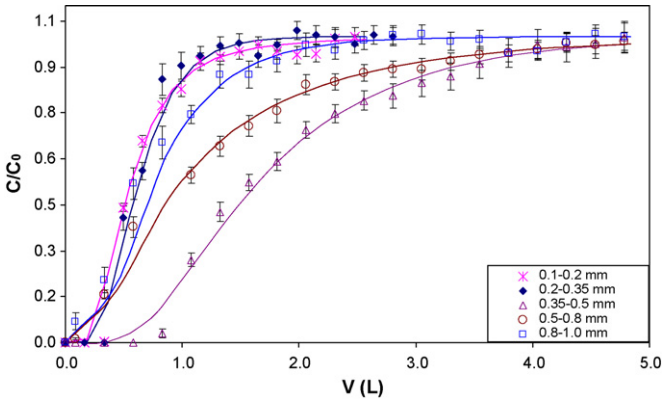


**Fig. 4.** The measured and modelled (continuous line) breakthrough curves for sorption of Cu(II) (70 mg $L^{-1}$) onto grape stalks at different particle sizes (0.1–0.2; 0.2–0.35; 0.35–0.5; 0.5–0.8 and 0.8–1.0 mm). Error bars represent one standard deviation.

The pH was monitoring as a function of time, the values measured were ranging between 5.5 at starting point of the experiment and 4 when the column was exhausted; the pH decreased as a consequence of cations and protons release and confirms the ion exchange as a most important mechanism in the metal sorption on the grape stalk wastes.

Batch experiments were performed in a previous study and the maximum sorbent capacity was determined by the Langmuir isotherm model [11]. The value reported in that work for Cu(II) onto grape stalk wastes was 10.2 g $kg^{-1}$. This value can be compared to those obtained in this study in column experiments. Tables 2 and 4 report the bed capacity for the Cu(II) at two inlet concentrations and at different particle sizes, respectively. It can be observed that batch parameter is lower than the values observed in column operation. However, it is necessary to pointing out that the particle size used in batch experiments was larger than those used in this study and the methodologies used to obtain the sorbent capacity in batch and column experiments are different.

Gupta reported bed capacities for Cu(II) removal from aqueous solutions by activated slag [7]. The column capacity reported was 38 g $kg^{-1}$, for an inlet Cu(II) concentration of 250 mg $L^{-1}$. This value denotes that bed capacities obtained in this study (Tables 2 and 4) are competitive compared to the values reported in literature for other type of sorbents.

### 3.5. Desorption experiments

Desorption flow experiments were conducted after Cu(II) column saturation under the conditions mentioned in Section 2.4. The amount of contaminant desorbed was calculated as the area under the elution curve [32].

Fig. 5 shows the Cu(II) desorption profile $C_e$ (mg $L^{-1}$) after sorption step at different initial concentration. It is observed that 0.030 and 0.040 L of elution solution were sufficient for almost complete desorption for 20 and 70 mg $L^{-1}$ of Cu(II), respectively. The first aliquot of 0.015 L elutes 56% of the sorbed amount for both inlet concentrations columns, and the rest is desorbed with additional 0.1 L of elution solution. The percentage recovery was 85% for both Cu(II) inlet concentrations.

## 4. Conclusions

The results show that grape stalk waste can be employed as sorbent for the removal of Cu(II) from aqueous solutions in column

**Table 4**
Effect of the particle size on the fixed-bed calculations and breakthrough capacity for Cu(II) sorption onto grape stalks.

| Particle size | $L$ | $V_x$ | $V_b$ | $t_x$ | $t_f$ | $q_{column}$ | $\delta$ |
|---|---|---|---|---|---|---|---|
| 0.1–0.2 mm | 6.0 | 1.16 | 0.33 | 105 | 10 | 14.10 | 4.7 |
| 0.2–0.35 mm | 6.2 | 0.99 | 0.33 | 90 | 10 | 14.76 | 4.5 |
| 0.35–0.5 mm | 6.5 | 3.30 | 0.83 | 300 | 20 | 49.24 | 5.3 |
| 0.5–0.8 mm | 6.7 | 3.20 | 0.38 | 291 | 4 | 48.43 | 5.2 |
| 0.8–1.0 mm | 6.8 | 1.57 | 0.31 | 143 | 1.8 | 36.46 | 4.9 |

**Table 5**
Effect of the particle size on the physical parameters obtained and model parameters obtained by fitting Cu(II) experimental breakthrough data to the non-equilibrium sorption model.

| Particle size | Physical parameters ($R = 1$) | | | Two-site sorption model parameters | | | | | |
|---|---|---|---|---|---|---|---|---|---|
| | $D$ | $v$ | $r^2$ | $R$ | $\beta$ | $\omega$ | $r^2$ | $k_L$ | $\alpha$ |
| 0.1–0.2 mm | 2.4 | 3.0 | 0.978 | 30 | 0.90 | 0.09 | 0.980 | 0.02 | 0.015 |
| 0.2–0.35 mm | 1.6 | 2.5 | 0.977 | 25 | 0.90 | 0.09 | 0.980 | 0.02 | 0.015 |
| 0.35–0.5 mm | 4.5 | 3.8 | 0.993 | 92 | 0.85 | 0.21 | 0.989 | 0.07 | 0.009 |
| 0.5–0.8 mm | 5.4 | 1.9 | 0.989 | 44 | 0.72 | 0.03 | 0.980 | 0.03 | 0.001 |
| 0.8–1.0 mm | 3.0 | 2.2 | 0.974 | 42 | 0.51 | 0.05 | 0.964 | 0.03 | 0.001 |

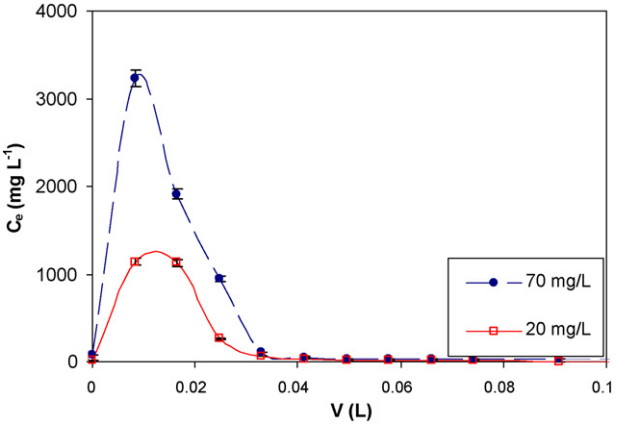


**Fig. 5.** Cu(II) desorption profile after sorption step at different initial concentration (20 and 70 mg $L^{-1}$) obtained by using 0.1 M $HClO_4$ solution as eluent. Error bars represent one standard deviation.

experiments. It is also showed that the two-site sorption model describes satisfactorily the mobility of Cu(II) ions in grape stalk wastes.

The sorption capacity is depending on the inlet Cu(II) ion concentration, at the highest Cu(II) concentration (70 mg $L^{-1}$) the grape stalks column saturated quickly leading to earlier breakthrough and exhaustion time.

The transport, bed capacity and sorption parameters are affected by the particle sizes. It is found that for the large particle size (larger than 0.35 mm) the parameters obtained by the two-site non-equilibrium decreased with increasing particle sizes. However, for small particle sizes (less than 0.35 mm) a high flow resistance of the column and reduced sorption capacities were obtained.

The metal recovery was close to 85% in the desorption experiments after Cu(II) sorption step at two inlet concentrations studied.

## Acknowledgments

The authors acknowledge the contribution of MICINN project CTM2008-06776-C02-02/TECNO (Spanish Ministry of Science and Innovation).

## References

[1] X. Li, Q. Xu, G. Han, W. Zhu, Z. Chen, X. He, X. Tian, Equilibrium and kinetic studies of copper(II) removal by three species of dead fungal biomasses, J. Hazard. Mater. 165 (2009) 469–474.
[2] H. Ucun, O. Aksakal, E. Yildiz, Copper(II) and zinc(II) biosorption on *Pinus sylvestris* L., J. Hazard. Mater. 161 (2009) 1040–1045.
[3] J. Febrianto, A.N. Kosasih, J. Sunarso, Y.-H. Ju, N. Indraswati, S. Ismadji, Equilibrium and kinetic studies in adsorption of heavy metals using biosorbent: a summary of recent studies, J. Hazard. Mater. 162 (2009) 616–645.
[4] J. Bouzid, Z. Elouear, M. Ksibi, M. Feki, A. Montiel, A study on removal characteristics of copper from aqueous solution by sewage sludge and pomace ashes, J. Hazard. Mater. 152 (2008) 838–845.
[5] I.A. Şengil, M. Özacar, H. Türkmenler, Kinetic and isotherm studies of Cu(II) biosorption onto valonia tannin resin, J. Hazard. Mater. 162 (2009) 1046–1052.
[6] T.A. Kurniawan, G.Y.S. Chan, W. Lo, S. Babel, Physico-chemical treatment techniques for wastewater laden with heavy metals, Chem. Eng. J. 118 (2006) 83–98.
[7] V.K. Gupta, Equilibrium uptake, sorption dynamics, process development, and column operations for the removal of copper and nickel from aqueous solution and wastewater using activated slag, a low-cost adsorbent, Ind. Eng. Chem. Res. 37 (1998) 192–202.
[8] I. Villaescusa, M. Martínez, N. Miralles, Heavy metal uptake from aqueous solution by cork and yohimbe bark wastes, J. Chem. Technol. Biotechnol. 75 (2000) 812–816.
[9] W. Li, H. Zhao, P.R. Teasdale, R. John, Preparation and characterization of a poly(acrylamidoglycolic acid-co-acrylamide)hydrogel for selective binding of $Cu^{2+}$ and application to diffuse gradients in thin films measurements, Polymer 43 (2002) 48303–54809.
[10] E. Malkoc, Y. Nuhoglu, Removal of Ni(II) ions from aqueous solutions using waste of tea factory: adsorption on a fixed-bed column, J. Hazard. Mater. 135 (2006) 328–336.
[11] I. Villaescusa, N. Fiol, M. Martínez, N. Miralles, J. Poch, J. Serarols, Removal of copper and nickel ions from aqueous solutions by grape stalks wastes, Water Res. 38 (2004) 992–1002.
[12] C. Escudero, C. Gabaldón, P. Marzal, I. Villaescusa, Effect of EDTA on divalent metal adsorption onto grape stalk and exhausted coffee wastes, J. Hazard. Mater. 152 (2008) 476–485.
[13] M. Martinez, N. Miralles, S. Hidalgo, N. Fiol, I. Villaescusa, J. Poch, Removal of lead(II) and cadmium(II) from aqueous solutions using grape stalk waste, J. Hazard. Mater. 133 (2006) 203–211.
[14] N. Fiol, C. Escudero, I. Villaescusa, Chromium sorption and Cr(VI) reduction to Cr(III) by grape stalks and yohimbe bark, Bioresour. Technol. 99 (2008) 5030–5036.
[15] B. Fonseca, A. Teixeira, H. Figueiredo, T. Tavares, Modelling of the Cr(VI) transport in typical soils of the north of Portugal, J. Hazard. Mater. (2009), doi:10.1016/j.jhazmat.2009.01.049.
[16] T.-H. Wang, M.-H. Li, S.-P. Teng, Bridging the gap between batch and column experiments: a case study of Cs adsorption on granite, J. Harzard. Mater. 161 (2009) 409–415.
[17] K.H. Chu, Improved fixed bed models for metal biosorption, Chem. Eng. J. 97 (2004) 233–239.
[18] N. Toride, F.J. Leij, M.T. van Genuchten, The CXTFIT Code for Estimating Transport Parameters from Laboratory or Field Tracer Experiments, 137, U.S. Salinity Laboratory, U.S. Department of Agriculture, Riverside, CA, 1995.
[19] D.R. Cameron, A. Klute, Convective–dispersive solute transport with a combined equilibrium and kinetic adsorption model, Water Resour. Res. 13 (1977) 183–188.
[20] D.C.W. Tsang, W. Zhang, I.M.C. Lo, Modeling cadmium transport in soils using sequential extraction, batch, and miscible displacement experiments, Soil Sci. Soc. Am. J. 71 (2007) 674–681.
[21] K. Bajracharya, D.A. Barry, MCMFIT—efficient optimal fitting of a generalized nonlinear advection-dispersion model to experimental-data, Comput. Geosci. 21 (1995) 61–76.
[22] S.K. Kamra, B. Lennartz, M.T. Van Genuchten, P. Widmoser, Evaluating non-equilibrium solute transport in small soil columns, J. Contam. Hydrol. 48 (2001) 189–212.
[23] M.T. van Genuchten, A closed-form equation for predicting the hydraulic conductivity of unsaturated soils, Soil Sci. Soc. Am. J. 44 (1980) 892–898.
[24] V.K. Gupta, S.K. Srivastava, D. Mohan, Equilibrium uptake, sorption dynamics, process optimization, and column operations for the removal and recovery of malachite green from wastewater using activated carbon and activated slag, Ind. Eng. Chem. Res. 36 (1997) 2207–2218.
[25] V.K. Gupta, S.K. Srivastava, R. Tyagi, Design parameters for the treatment of phenolic wastes by carbon columns (obtained from fertilizer waste material), Water Res. 34 (2000) 1543–1550.
[26] V.V. Goud, K. Mohanty, M.S. Rao, N.S. Jayakumar, Prediction of mass transfer coefficients in a packed bed using tamarind nut shell activated carbon to remove phenol, Chem. Eng. Technol. 28 (2005) 991–997.
[27] Y.S. Al-Degs, M.A.M. Khraisheh, S.J. Allen, M.N. Ahmad, Adsorption characteristics of reactive dyes in columns of activated carbon, J. Hazard. Mater. 165 (2009) 944–949.
[28] N.V. Farinella, G.D. Matos, M.A.Z. Arruda, Grape bagasse as a potential biosorbent of metals in effluent treatments, Bioresour. Technol. 98 (2007) 1940–1946.

[29] T.V.N. Padmesh, K. Vijayaraghavan, G. Sekaran, M. Velan, Batch and column studies on biosorption of acid dyes on fresh water macro alga *Azolla filiculoides*, J. Hazard. Mater. 125 (2005) 121–129.
[30] V.K.C. Lee, J.F. Porter, G. McKay, Development of fixed-bed adsorber correlation models, Ind. Eng. Chem. Res. 39 (2000) 2427–2433.
[31] M.J. Rivero, R. Ibanez, I.M. Ortiz, Mathematical modelling of styrene drying by adsorption onto activated alumina, Chem. Eng. Sci. 57 (2002) 2589–2592.
[32] P. Miretzky, C. Muñoz, A. Carrillo-Chávez, Experimental Zn(II) retention in a sandy loam soil by very small columns, Chemosphere 65 (2006) 2082–2089.